IEEE Access
Multidisciplinary ⋮ Rapid Review ⋮ Open Access Journal

Received June 16, 2021, accepted July 5, 2021, date of publication July 12, 2021, date of current version July 21, 2021.

Digital Object Identifier 10.1109/ACCESS.2021.3096264

Detection and Identification of Low-Slow-Small Rotor Unmanned Aerial Vehicle Using Micro-Doppler Information

GUANGYU JI[1], CHEN SONG[2], AND HONGTAO HUO[1], (Member, IEEE)
[1]Department of Information Technology and Cyber Security, People's Public Security University of China, Beijing 100038, China
[2]National Key Laboratory of Microwave Imaging Technology, Aerospace Information Research Institute, Chinese Academy of Sciences, Beijing 100190, China
Corresponding authors: Hongtao Huo (huohongtao@ppsuc.edu.cn) and Chen Song (songchen@aircas.ac.cn)

ABSTRACT The capability of a radar system to detect and identify the low-slow-small rotor unmanned aerial vehicle (UAV) is intensely important for management and control in low altitude, and it can be enhanced by the characteristics of UAV, which inherently carries micro-Doppler information. In this paper, we establish a micro-motion model of rotor UAV, and analyze the range walking and Doppler broadening caused by micro-motion. Hence, based on the characteristics of micro-Doppler of the rotors apart from the main body for the moving UAV, a micro-motion target detection and micro-Doppler parameters estimation method is proposed. Firstly, a method based on datashift in range dimension is used to compensate the translational component of the main body. Secondly, for the echo after translation compensation, a parameter estimation method of micro-Doppler based on the optimal demodulation operator is proposed. The operator contents the maximum likelihood criterion, which strengthens the difference between the micro-Doppler signal and the background clutters, so that more signal energy can be accumulated while the clutter is suppressed. Subsequently, the micro-Doppler parameters of the micro-motion component are obtained by the optimal demodulator, so that the detection and identification of the target are realized. Additionally, the performance of proposed method, including parameter estimation, signal-to-noise ratio (SNR) improvement and the calculation efficiency is analyzed. Finally, the simulation and experimental results reveal that the proposed method does possess the capability to improve the performance of detection and recognition of rotor UAV.

INDEX TERMS Micro-Doppler, unmanned aerial vehicle (UAV), optimal demodulation operator, micro-motion parameter estimation, micro-motion target detection and identification.

I. INTRODUCTION

With the rapid development of application in military, photography, agriculture, transportation and other fields, the number of low-altitude aircraft, typical of rotor UAV, has exploded [1]–[4]. The problems of air defense safety, flight safety and public safety caused by the ''illegal flight'' and ''runaway flight'' of consumer UAVs have always been a looming weakness in the air defense system of various countries, which is harmful to public security and even national security [5]. Low-altitude targets with ''low, slow, small'' features expressed invisible and inaudible character lead to a widespread problem, which has been formed a serious negative impact [6]. As a result, it is urgent to develop detection signal processing technology of low-altitude surveillance radar, which can improve the performance of detection, position and tracking of UAVs, and defend the public rights and flight safety.

Accurate detection is the premise of identification, tracking, and interception. The detection of UAVs has the following difficulties. Firstly, the UAV targets have the character of small Radar Cross Section (RCS), weak echo energy and slow velocity, which make it difficult to be detected, for the radar echo signal of UAV targets is submerged in the clutter signal or noise signal easily [7]. Secondly, although the clutter component of the radar sampling unit can be reduced by improving the range resolution of the radar, and the target detection probability can be improved to a certain extent,

The associate editor coordinating the review of this manuscript and approving it for publication was Mehmet Alper Uslu.

the additional Doppler modulation caused by the rotation of rotor on the UAV result in the micro motion of the target, which widen the Doppler domain, disperse the target energy, and reduce the detection probability [8]. In fact, the periodic Doppler modulation caused by the rotation of UAV's rotor in the echo, namely micro-Doppler, can be used as a unique feature of UAV, which is helpful to its identification. Meanwhile, by estimating the micro-Doppler parameters of UAV targets in the detection process and compensating it in the echo signal, the more concentrated energy of UAV targets and higher signal-to-noise ratio (SNR) would be get, so that the detection performance of the UAVs would be improved.

At present, many scholars have studied the RCS characteristics of ''low-slow-small'' targets represented by various UAVs. The research is focused on the difference of echo power or RCS characteristics caused by the difference of motion characteristics between UAV main body translation and its rotor rotation for the detection of ''low-slow-small'' targets [9]. The echo of rotor UAV mainly includes two kinds of components [10]: one is the translational component generated by the motion of UAV itself, which can be modeled by polynomial phase signal (PPS) ; the other is the micro-Doppler component, which is generated by the rotation of rotor, whose echo is a typical sine frequency modulation (SFM) signal. These two components make up the combination of PPS-SFM in the echo, and this kind of target has become the focus of low altitude detection. For the parameter estimation and feature extraction of this mixed combination, effective separation methods are mainly based on signal features or time-frequency features. The former utilizes the difference in the models two components. Typical high-order statistical methods, such as high-order ambiguity functions [11], require a higher SNR. This type of method has difficulties when the signal is weak. The delay conjugate multiplication method [12] and the phase compensation function method [13] need to know some prior information, such as the order of the target movement, etc., which turn out to be complex operation process. In the latter, the time-frequency analysis of the signal is done first. Then the envelope walk compensation and phase compensation of the time-frequency signal is completed. However, traditional time-frequency analysis methods, such as short-time Fourier transform (STFT) [14], Wigner-Ville Distribution (WVD) [15], Radon-Wigner Transform (RWT) [16], Wigner-Hough Transform (WHT) [17], etc., not only require a high SNR, but also is limited by many factors, including the resolution of the time-frequency distribution, the accuracy of peak extraction and the accuracy of polynomial fitting, etc.. In addition, when detecting multiple targets, there exist cross components which will conceal the signal of weak targets [18]. The method of Radon transform with fractional Fourier transform (FrFT) [19] or short time fractional Fourier transform (STFrFT) [20] may lead to low estimation accuracy due to multi-layer transmission error and even motion order estimation error. In [21], Hilbert-Huang Transform (HHT) method is utilized to extract the micro-Doppler component. Yet this method is only effective for micro-Doppler signals without frequency overlapping. For target with multi-component of micro-motion, the characteristic curve cannot be separated because of overlapping in time-frequency plane, which leads to poor precision of parameter estimation.

Regarding the above-mentioned problem of achieving target detection and parameter estimation in the mixed signal, this paper takes the rotor UAV as the research target, analyzes the characteristics of electromagnetic scattering close to the reality, and constructs the motion model of UAV with micro-Doppler component generated by rotor rotation. For the echo of the UAV in motion, firstly, this paper proposes a method based on the range shift of the target's translational compensation, which can accurately extract the target's translational parameters and separate the two components of translational and micro-movement. Secondly, using the method of maximum likelihood estimation, this paper proposes a method of estimating the parameters of the micro-Doppler based on the optimal estimation of the demodulation operator. After compensating for the translational movement of the target, the optimal demodulation operator is used to enhance the difference between the characteristics of the background clutter and the micro-Doppler signal, and increase the energy concentration of the micro-motion component, thereby effectively improving the SNR of the target. In this way, the detection performance of the radar is improved. Finally, the performance of detection and parameter estimation of the proposed algorithm is analyzed by simulation and measured data. The results verify the effectiveness of the method. The method proposed in this paper is not limited by the type of noise. It can estimate the parameters of multiple targets simultaneously and avoid the influence of error transmission. At the same time, the precision of micro-motion parameters obtained by this method is improved, which can be widely used in the detection or recognition of rotor UAV.

The structure of this paper is as follows: in Section II, the model of micro motion target of rotor UAV is established. In Section III, the method of detection and parameter estimation of micro motion target is proposed. In Section IV, the proposed method is tested and verified by simulation and measured data. Section V is summarized and prospect.

II. MODEL OF MICRO-MOTION TARGET SIGNAL

Using point scattering function to model micro-motion target, a three-dimensional Cartesian coordinate system is established as Fig.1. Suppose the radar is located at the origin of the coordinate system, denoted as point O. The distance between center of a rotor C and radar is R_c. Point C moves with the main body of UAV as a part of it. During the sampling time of echo, the UAV movement could be approximately regarded as uniform rectilinear motion. Thus, the distance between radar

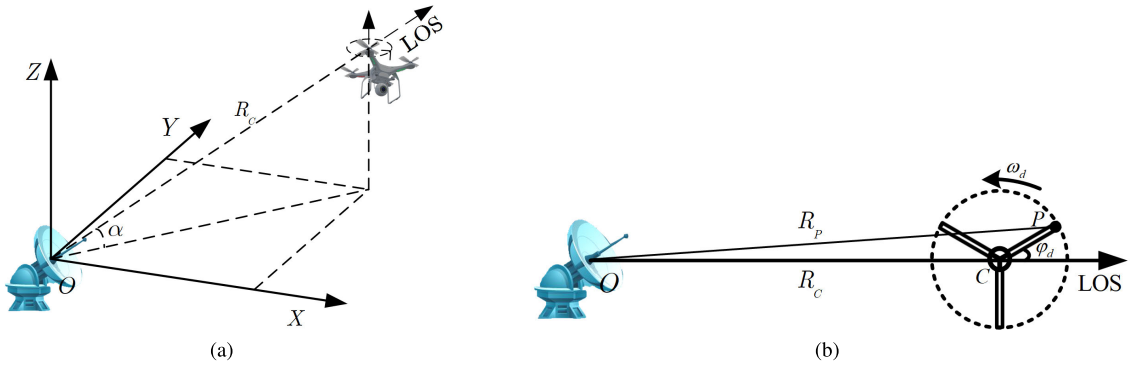

FIGURE 1. Geometric relationship between radar and rotor UAV. (a) Geometric diagram of rotor UAV and radar in three-dimensional cartesian coordinate system, (b) Geometric diagram of rotor and radar in the plane projected in the line-of-sight direction of radar.

and point C can be expressed as

$$R_c(t_n) = R_0 + v_C t_n, \tag{1}$$

where v_c is the projection of UAV's velocity in the line-of-sight direction of radar, t_n is slow time, R_0 is the distance between C and radar at the initial sampling moment.

Supposing P is a strong scattering point on the rotor and the distance between P and C is l ($l \ll R_c$). Usually, the edge of the rotor is an obvious strong scattering point that can be detected, which is generally determined by the material, shape and size of the rotor. Therefore, it is reasonable to express P as the scattering point located at the edge of the rotor, and then l can be regarded as the length of the rotor. The slant range of P is

$$R_p(t_n) = R_c(t_n) + l\cos(\omega_d t_n + \phi_d), \tag{2}$$

where ω_d is the projection of angular velocity of scattering point P rotating around rotor center C in the line-of-sight direction of radar, ϕ_d is the initial rotation angle of P. It should be noted that since the rotor UAV detected and identified in this paper is located at low altitude area in most cases, the radar observation elevation angle is generally less than 10°, the difference of the rotation angular velocity of P in the horizontal direction and its projection of radar line-of-sight direction is merely less than 2%. Therefore, it can be approximately considered that ω_d is the angular velocity of scattering point P rotating around C.

When radar transmits Linear Frequency Modulation (LFM) signal, the received echo of scattering point P is expressed as

$$s(t_m, t_n) = \sigma_P \mathrm{rect}\left(\frac{t_m - 2R_P/c}{T}\right) \times \exp\left[j2\pi f_c\left(t_m - \frac{2R_P}{c}\right) + j\pi K\left(t_m - \frac{2R_P}{c}\right)^2\right], \tag{3}$$

where σ_P is scattering coefficient of P, rect$(\cdot)$ is rectangular envelope function, c is velocity of electromagnetic wave propagation, T is pulse width, f_c is carrier frequency of signal, K is frequency modulation slope of signal, t_m and t_n are fast time and slow time respectively. The echo is processed by Dechirp, which is a common method to realize pulse compression in the area of radar signal processing. After dechirp processing, the slope range between target and the reference range is represented by beat signal as

$$S_d(f, t_n) = \sigma_P T \mathrm{sinc}\left\{T\left[f - \frac{2K}{c}(R_P - R_{\mathrm{ref}})\right]\right\} \exp\left[-j\frac{4\pi}{\lambda}(R_P - R_{\mathrm{ref}})\right] \exp\left[j\frac{4\pi K}{c^2}\left(R_P^2 - R_{\mathrm{ref}}^2\right)\right] \exp\left\{j\frac{4\pi R_{\mathrm{ref}}}{c}\left[f - \frac{2K}{c}(R_P - R_{\mathrm{ref}})\right]\right\}, \tag{4}$$

where R_{ref} is the reference range selected in the dechirp processing, f is difference frequency, corresponding to the range between target and reference range, λ is the wavelength.

In (4), there are three phase terms. The first term contains the phase history of target, from which the micro-Doppler information of target can be extracted. The second term indicates the "oblique" term of echo envelope. When the difference frequency matches the target range, the value of sinc term is 1, which means that this phase term has nothing to do with target range and fails to affect the measurement result. The third term is called Residual Video Phase (RVP) term, which can be removed by corresponding means [22]. After processing, we can substitute (1) (2) into (4) and obtain the expression of micro-Doppler in the slow time domain of P as

$$S_d(t_n) = \psi_d \exp\{j[\kappa_d t_n + \rho_d \cos(\omega_d t_n + \varphi_d)]\}, \tag{5}$$

where $\psi_d = \sigma_P T \exp[-j4\pi(R_0 - R_{\mathrm{ref}})/\lambda]$, containing scattering information of P. In the phase term of (5), $\kappa_d = -4\pi v_C/\lambda$ contains translational information of P with UAV as a whole, $\rho_d = -4\pi l/\lambda$ contains information of the length between P and rotation center C, and the cosine term contains the information of angular velocity and initial phase of P.

Equation (5) describes the micro-Doppler effect caused by the rotation of scattering points on the rotor in the slow-time domain. By estimating the parameters of each micro-motion

component, the rotation frequency and the length of the rotor can be obtained, and then the UAV can be detected and identified.

III. METHOD OF UAV TARGET DETECTION AND PARAMETERS ESTIMATION

A. TRANSLATIONAL COMPONENT COMPENSATION

When UAV is flying, the modulation characteristic of micro motion caused by rotor rotation is shown as SFM signal in the echo. When UAV has translational motion caused by its own flight, the PPS signal will be superimposed on the echo due to the translational modulation. Virtually, the signal with uncompensated translational motion or compensated one using only roughly measured data is a mixed form of LFM-SFM. Due to the existence of translational component, the echo of the target will cross the range gate in the slow-time domain as a whole, and the periodicity of micro-Doppler characteristics will be destroyed, resulting in the failure of current parameter estimation methods. Moreover, translational component will broaden the difference frequency spectrum, which lead to a more data accumulation in the differential frequency domain, if micro-Doppler information need to be collected completely. However, this will increase the amount of computation and put forward higher requirements for the sampling rate of system and the bandwidth of detector. Therefore, it is necessary to estimate the parameter of translational component accurately and compensate it first.

The translational motion of UAV usually has the characteristics of high maneuverability, especially for some small consumer UAVs. Combined with the actual scope of rotor rotation speed of UAV during flight, high PRF signal is transmitted for echo data acquisition. It can be seen that in a relatively short period of time, echo data of target with enough period can be obtained for analysis. During this period, the translational movement speed of UAV changes sufficiently small that it can be regarded as a uniform movement. Therefore, the motion model of (1) can be used to analyze the translational motion of UAV.

Taking (4) as the manifestation of the echo signal in the range-slowtime domain, it is compensated for translational component. The compensation is divided into two parts, namely envelope compensation and phase compensation. Envelope compensation is to compensate the translational motion of the target to the same range gate in slow time, and phase compensation is to compensate the phase term of the translational component in the target.

For the envelope compensation of translational component, transform mapping method is used, such as Keystone transform [23], Radon transform [24]. And so is angle rotation method of signal space [25], etc. The purpose of these methods is to correct the translational component across multiple range gates to the same gate. However, the former method will decrease the efficiency of operation, because in the process of transformation, either it needs to complete two-dimensional interpolation, or it cannot use FFT directly. For the latter method, in the process of rotation, when the speed of translational motion is fast enough, the rotation angle will be large, which will lead to distortion of the micro-motion component after rotation and affect the estimation of micro-motion parameters and matching result.

To solve this problem, this paper uses the method of datashift in range dimension to realize translational envelope compensation. Specifically, let differential frequency axis f in (4) be mapped to f' with $f' = f - 2Kvt_n/c$. Meanwhile, let v be searched with a certain initial value and step size. When the accumulated energy R_d shown as (7) reach the maximum in the Doppler domain, the corresponding v is the estimated translational velocity v_C. The mechanism of the method described above can be shown in Fig. 2. The expression of v_C is

$$v_C = \arg\max_v \left[\max |R_d(f, f_n; v)|^2\right], \tag{6}$$

where

$$R_d(f, f_n; v) = \int_{-\infty}^{+\infty} S_d\left(f + \frac{2Kvt_n}{c}, t_n\right) g_\sigma\left(\frac{t_n}{T_n}\right) \exp(j2\pi f_n t_n)\, \mathrm{d}t_n \tag{7}$$

$$g_\sigma(t) = \begin{cases} 1, & 0 \leqslant t < 1 \\ 0. & \text{otherwise} \end{cases}$$

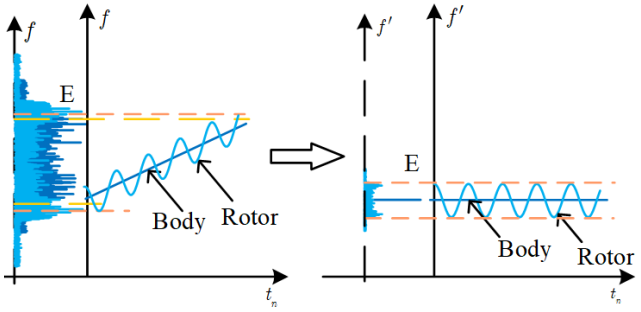

FIGURE 2. Mechanism of datashift in range dimension method.

In (6)(7), T_n denotes the slow-time window of processed data, f_n denotes the Doppler frequency which is obtained by Fourier transform of slow time t_n.

Usually in the process of radar searching for UAV, low Pulse Repetition Frequency (PRF), narrow bandwidth signal with multi-angular scanning is used first. After obtaining the approximate position and velocity of suspicious target, high PRF, wideband signal with small scope scanning should be used to search in detail. The latter search mode can deal with targets with micro-Doppler characteristics, which is the content of interest in this paper. The approximate position and translational velocity acquired in the former search mode could be substituted into the method in this subsection as a initial value. Then reasonable search step size set from the bandwidth, PRF and other parameters of signal is used for

iteration, so as to quickly obtain the accurate translational velocity of target.

Aftering obtaining the translational velocity v_C of target, let v_C be a parameter to compensate the translational component in the signal of (4). Then the expression of micro-Doppler could be obtained as

$$S_d\left(t_n\right) = \psi_d \exp\left[j\rho_d \cos\left(\omega_d t_n + \varphi_d\right)\right]. \tag{8}$$

Equation (8) is the expression of micro-Doppler after compensating translational component of (5).

B. OPTIMAL DEMODULATION OPERATOR

Discretely sampling the expression of micro motion in (8) in the slow-time domain with sampling point N, the micro-motion vector $\boldsymbol{S}_d$ is shown as

$$\boldsymbol{S}_d = \begin{bmatrix} \exp\left[j\rho_d \cos\left(\omega_d \times \Delta t + \varphi_d\right)\right] \\ \vdots \\ \exp\left[j\rho_d \cos\left(\omega_d \times (N-1)\,\Delta t + \varphi_d\right)\right] \end{bmatrix}, \tag{9}$$

where Δt is pulse repetition interval. According to the micro-motion characteristics of target in the radar echo, the observation equation is constructed as

$$\boldsymbol{X} = \psi_d \boldsymbol{S}_d + \boldsymbol{\varepsilon}, \tag{10}$$

where, $\boldsymbol{X} = \left[x_d\left(0\right), \ldots, x_d\left(N-1\right)\right]^{\mathrm{T}}$ is observed vector, $\boldsymbol{\varepsilon} = \left[\varepsilon\left(0\right), \ldots, \varepsilon\left(N-1\right)\right]^{\mathrm{T}}$ is noise vector. $\varepsilon\left(k\right) \sim \left(0, \sigma^2\right)$ is additive Gaussian white noise, whose covariance matrix is $\mathbf{R} = \sigma^2\mathbf{I}$. ψ_d is the scattering coefficient of the corresponding scattering point. Using maximum likelyhood estimation (MLE) method, the log likelyhood function of observed vector $\boldsymbol{X}$ is

$$\ln\left(L\left(\sigma^2 \left| \boldsymbol{X}\right.\right)\right) = -\frac{N}{2}\ln\left(2\pi\right) - N\ln\sigma - \frac{1}{2\sigma^2}\left(\boldsymbol{X} - \psi_d\boldsymbol{S}_d\right)^{\mathrm{H}}\left(\boldsymbol{X} - \psi_d\boldsymbol{S}_d\right). \tag{11}$$

Differentiating (11) with respect to σ^2, equating it to zero, the MLE of σ^2 could be obtained as

$$\hat{\sigma}^2 = \frac{1}{N}\left(\boldsymbol{X} - \psi_d\boldsymbol{S}_d\right)^{\mathrm{H}}\left(\boldsymbol{X} - \psi_d\boldsymbol{S}_d\right). \tag{12}$$

In (12), ψ_d and the other three parameters in the vector $\boldsymbol{S}$ (see (9)) are unknown fixed value and need to be estimated. The estimation result should minimize the variance of Gaussian white noise in each slow-time sampling of observation equation. Let $\boldsymbol{S} = \left[S\left(0\right), \ldots, S\left(N-1\right)\right]^{\mathrm{T}}$, where $S\left(k\right) = \exp\left[j\rho\cos\left(\omega k + \varphi\right)\right]$, $k = 0, 1, \ldots, N-1$. Then the estimated value of the four parameters could be expressed as

$$\left(\hat{\rho}_d, \hat{\omega}_d, \hat{\varphi}_d, \hat{\psi}_d\right) = \underset{(\rho,\omega,\varphi,\psi)}{\arg\min}\left[\left(\boldsymbol{X} - \psi\boldsymbol{S}\right)^{\mathrm{H}}\left(\boldsymbol{X} - \psi\boldsymbol{S}\right)\right]. \tag{13}$$

ϕ_d can be estimated by maximum likelyhood estimation. That is, let the derivative of (13) with respect to ψ equal zero, the MLE of ψ_d could be

$$\hat{\psi}_d = \frac{\boldsymbol{S}^{\mathrm{H}}\boldsymbol{X}}{N}. \tag{14}$$

Then substituting (14) into (13), we can obtain

$$\begin{aligned}\left(\hat{\rho}_d, \hat{\omega}_d, \hat{\varphi}_d\right) &= \underset{(\rho,\omega,\varphi)}{\arg\min}\left(\boldsymbol{X}^{\mathrm{H}}\boldsymbol{X} - \frac{1}{N}\left|\boldsymbol{S}^{\mathrm{H}}\boldsymbol{X}\right|^2\right) \\ &= \underset{(\rho,\omega,\varphi)}{\arg\max}\left|\boldsymbol{S}^{\mathrm{H}}\boldsymbol{X}\right|^2 \\ &= \underset{(\rho,\omega,\varphi)}{\arg\max}\left|\sum_{k=0}^{N-1} x_d\left(k\right)\phi\left(k\right)\right|^2,\end{aligned} \tag{15}$$

where $\phi\left(k\right)$ is called demodulation operator, whose expression is defined as

$$\phi\left(k\right) = S^*\left(k\right) \overset{\text{def}}{=} \exp\left[-j\rho\cos\left(\omega k\Delta t + \varphi\right)\right]. \tag{16}$$

The demodulation operator $\phi\left(k\right)$ makes full use of the similarity with the micro-Doppler component of signal, and its performation is optimal when sufficient data is observed. The physical meaning of $\phi\left(k\right)$ can be equivalent to: The more $\phi\left(k\right)$ matches the real micro-Doppler characteristics of signal in the echo, the higher the energy is concentrated after demodulating in the transform domain. If and only if the parameters in $\phi\left(k\right)$ are equal to the real micro-Doppler parameters of signal, namely $\rho = \rho_d, \omega = \omega_d, \varphi = \varphi_d$, the energy reaches the largest value. For proof of this, see section III-D1 for details.

C. TARGET DETECTION

In the hypothetical test, let H_0 be the non-existence of micro-motion target and H_1 be the existence of micro-motion target. Then the observation model of two hypotheses are

$$\begin{aligned} H_0 &: \boldsymbol{X} = \varepsilon, \\ H_1 &: \boldsymbol{X} = \psi_d\boldsymbol{S}_d + \varepsilon. \end{aligned} \tag{17}$$

Let D be the test statistic of target detection:

$$D = \left|\boldsymbol{S}^{\mathrm{H}}\boldsymbol{X}\right|^2 = \left|\sum_{k=0}^{N-1} x_d\left(k\right)\phi\left(k\right)\right|^2. \tag{18}$$

It can be seen from (18) that the test statistic D is square law detection of the observed vector after demodulation. Therefore, each sampling unit of test statistic is subject to exponential distribution whose probability density function (PDF) is

$$f_D\left(x\right) = \frac{1}{\lambda'}\exp\left(-\frac{x}{\lambda'}\right), \quad x \geqslant 0, \tag{19}$$

where λ' is average power and it can be expressed as

$$\lambda' = \begin{cases} \mu, & H_0 \\ \mu\left(1+\lambda\right), & H_1. \end{cases} \tag{20}$$

In other word, the total noise power level is μ under H_0 hypothesis, compared with $\mu\left(1+\lambda\right)$ under H_1 hypothesis, where λ is the average power rate of signal and noise.

Constant false alarm rate (CFAR) method [26] is often used in radar target detection, which can find target while the probability of false alarm rate remains fixed. We need to use the sliding window method to estimate the noise power of

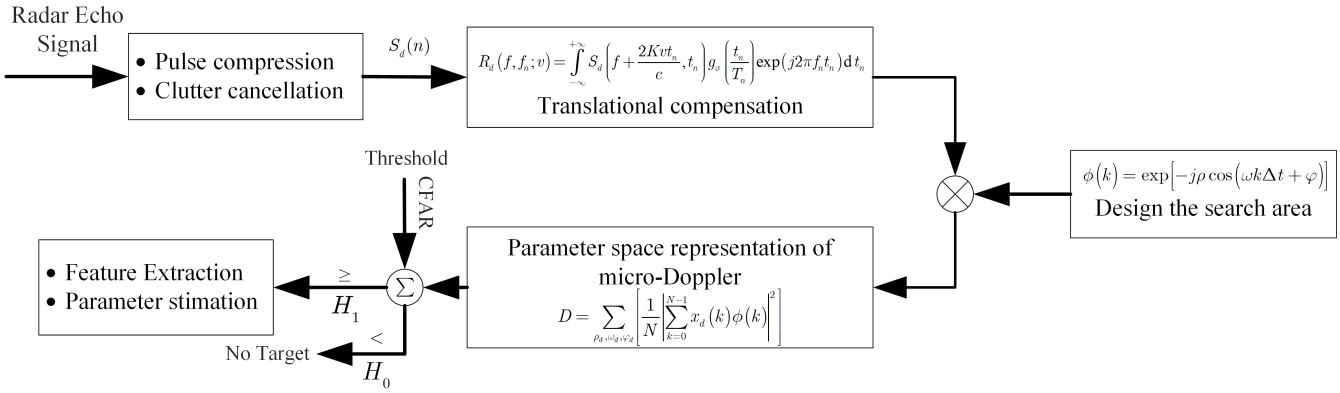

FIGURE 3. Structure of optimal detection system.

background in each sampling unit of the test statistics, and then calculate the threshold T for target detection according to the preset false alarm rate P_{fa} to make following judgments:

$$D \underset{H_0}{\overset{H_1}{\gtrless}} T. \tag{21}$$

It should be noted that using different kind of CFAR method on sampling unit will obtain different value of threshold, which will also reflect the performance of each method. The performance comparison of different CFAR methods is not main research content of this paper, so it is omitted here.

According to the judgement of the optimal detection of micro-Doppler component in radar echo, the structure of optimal detection system is designed, as shown in Fig. 3.

D. PERFORMANCE OF METHOD

1) PERFORMANCE OF TARGET MICRO-MOTION PARAMETER ESTIMATION

It has been mentioned in section III-B that by selecting appropriate parameters of (ρ, ω, φ) in the demodulation operator $\phi(k)$ so that the demodulated observation of micro-motion target can obtain optimal energy concentration, a higher degree of discrimination of two hypothesis in the test statistics could be obtained. Substituting (9)(10)(16) into (18), the test statistics can be expressed as

$$D = \left| \psi_d \sum_{k=0}^{N-1} \exp\left[j\rho_d \cos\left(\omega_d k\Delta t + \varphi_d\right)\right] \times \exp\left[-j\rho\cos\left(\omega k\Delta t+\varphi\right)\right] + \sum_{k=0}^{N-1} \varepsilon(k)\phi(k) \right|^2. \tag{22}$$

The two terms in the absolute value of (22) are summation term after demodulation of signal and noise respectively. The signal summation term which can make H_0 and H_1 judgement to obtain higher discrimination is concerned here. It can be expressed as

$$D_1 = \psi_d \sum_{k=0}^{N-1} \exp\left[j\rho_d \cos\left(\omega_d k\Delta t + \varphi_d\right)\right] \times \exp\left[-j\rho\cos\left(\omega k\Delta t+\varphi\right)\right]. \tag{23}$$

After deduction and demonstration shown in Appendix A, we obtain

$$D_1 = \psi_d \sum_{k=0}^{N-1} J_0\left(2\rho_d \cos\left(\frac{\omega_d-\omega}{2}k\Delta t + \frac{\varphi_d-\varphi}{2}+\frac{\pi}{2}\right)\right) \times J_0\left(\rho_d-\rho\right)+\xi. \tag{24}$$

In (24), ξ is residual term, including a series of summation terms of the product of Bessel function above first order and corresponding cosine function. As demonstrated in Appendix A, when the PRF of radar signal get a large value, it will fail to form energy accumulation in the residual term ξ near the position of $(\rho_d, \omega_d, \varphi_d)$, thus D_1 can be expressed as

$$D_1 \doteq \psi_d \sum_{k=0}^{N-1} J_0\left(2\rho_d \cos\left(\frac{\omega_d-\omega}{2}k\Delta t + \frac{\varphi_d-\varphi}{2}+\frac{\pi}{2}\right)\right) \times J_0\left(\rho_d-\rho\right). \tag{25}$$

From the property of zero-order Bessel function of the first kind, it can be seen that the impulse response peak of D_1 will appear at the position of $(\rho_d, \omega_d, \varphi_d)$ in the parameter space (ρ, ω, φ), so that the test statistic D will obtain the highest level of discrimination between H_0 and H_1 hypotheses.

2) PERFORMANCE OF SIGNAL-TO-NOISE RATIO IMPROVEMENT

The improvement of signal-to-noise ratio (SNR) of the test statistic D after demodulation by the operator $\phi(k)$ when the parameters are matched under H_1 hypothesis (that is, the optimal parameter estimate is obtained) is helpful to improve the target detection performance. According to (25), when the parameters in the signal term are matched, namely

$\rho = \rho_d, \omega = \omega_d, \varphi = \varphi_d$ is established, a gain of N times couble be obtained in D_1. For the noise term, it can be seen from (22) that the demodulated noise term is expressed as

$$\begin{aligned}\varepsilon' &= \sum_{k=0}^{N-1} \varepsilon(k)\,\phi(k) \\ &= \sum_{k=0}^{N-1} \varepsilon(k) \exp\left[-j\rho\cos\left(\omega k\Delta t + \varphi\right)\right]. \end{aligned} \tag{26}$$

It is shown that the noise term after demodulation is noise multiplied by a number whose modulus is 1. Since $\varepsilon(k)$ and $\phi(k)$ are independent of each other, it does not form an energy cumulative effect for the summation of noise term ε' after demodulation. Therefore, when H_1 hypothesis is judged with parameters matched, the SNR of D is increased by N times of the original signal, which will significantly improve the target detection performance.

3) CALCULATION EFFICIENCY

According to the previous analysis, if the three parameters $(\rho_d, \omega_d, \varphi_d)$ are known, the calculation of demodulation operator will consume N times of complex multiplication and $N-1$ times of complex addition. However, all the three parameters are unknown and should be actually estimated. Therefore, it is necessary to utilize the parameter space for optimal estimation in order to obtain more accurate results, which requires a search assignment involving a three-dimension parameter space. Supposing the size of three direction of parameter space is N_ρ, N_ω and N_φ respectively, the total calculation is $N_\rho \cdot N_\omega \cdot N_\varphi \cdot N$ times of complex multiplication and $N_\rho \cdot N_\omega \cdot N_\varphi \cdot (N-1)$ times of complex addition if the optimal estimation is achieved, which will cost a lot of calculations. In this case, some ways to improve efficiency should be considered. According to extensive investigations and tests, prior knowledge of rotor UAV as ''low-slow-small'' target can be obtained, such as the rotation speed of rotor with 50–120 r/s and blade length of rotor with 8–15 cm, which can constraint the set range of the parameter space (ρ, ω, φ) in the proposed method in order to decrease the calculation amount. In addition, GPU parallel processing can be used on the hardware to further improve operating efficiency, which can satisfy the real-time requirement.

E. ALGORITHM

After the analysis above, The detection and identification method of rotor UAV is shown in Algorithm 1 and described as follow:

Supposing there are continuous echo signal sequences sampled into processor, in the first step, select N continuous echo samples and preprocess them, including pulse compression in dechirp method, clutter suppression in MTD, and then obtain the echo signal sequence $x(k), k = 1, \ldots, N$. In order to reduce the influence of the fixed clutter and background noise and keep the uniform motion approximation of target, the length N of sample amount for process per iteration cannot be too long or too short. In this paper, $N = 128$ is selected.

Algorithm 1 Target Detection and Parameter Estimation of Rotor UAV

Initialization: $i = 0$,
$\rho \in [\rho_{\min}, \rho_{\max}], \omega \in [\omega_{\min}, \omega_{\max}], \varphi \in [0, 2\pi]$
Input: sampled echo signal sequences
Output: $\hat{l}_d = \frac{\hat{\rho}_d \lambda}{4\pi}, \hat{\omega}_d, \hat{\varphi}_d$.
for $i - th$ **step:**
(1) Select N continuous echo samples from the input echo signal sequence and preprocess them, including pulse compression, clutter suppression in MTD;
(2) Compensate the translational component;
(3) Search $\left(\hat{\rho}_d, \hat{\omega}_d, \hat{\varphi}_d\right)$ in $\Theta_{(\rho,\omega,\varphi)}$ to maximize $\mathbf{\Gamma}(\rho, \omega, \varphi) = \left|\sum_{k=0}^{N-1} x_d(k)\,\phi(k; \rho, \omega, \varphi)\right|^2$, and set $D = \mathbf{\Gamma}\left(\hat{\rho}_d, \hat{\omega}_d, \hat{\varphi}_d\right)$;
(4) CFAR detection,
if $D \geq \mathrm{th}_{\mathrm{CFAR}}$, rotor UAV exists, then output rotor parameters and update searching range of $\Theta_{(\rho,\omega,\varphi)}$,
if $D \leq \mathrm{th}_{\mathrm{CFAR}}$, rotor UAV non-exists,
$i = i + 1$, go to next iteration.
End

In the second step, obtain the rough position of target and compensate the envelope of translational component using range dimension datashift method detailed in section III-A. The translational velocity for searching and the rough position of target can be initially set by previous detection with low PRF and narrow bandwidth signal and updated by the result from last iteration. After compensation processing, accumulate the echo signal near the position of target in the range dimension and compensate the phase term of translational component in order to form the observation signal $x_d(k), k = 1, \ldots, N$ for the next step.

In the third step, construct the parameter space $\Theta_{(\rho,\omega,\varphi)}$ and set the search accuracy and range of parameters, namely ρ, ω and φ. Based on engineering experience and prior knowledges, we set $\rho \in [\rho_{\min}, \rho_{\max}]$, $\omega \in [\omega_{\min}, \omega_{\max}]$, $\varphi \in [0, 2\pi)$, and the total number of search for ρ,ω,φ is U,V,Q, respectively. Then using the parameter space of $U \times V \times Q$ size, construct the demodulator $\phi(k; \rho, \omega, \varphi) = \exp\left[-j\rho\cos\left(\omega k\Delta t + \varphi\right)\right]$ and calculate $\mathbf{\Gamma}(\rho, \omega, \varphi) = \left|\sum_{k=0}^{N-1} x_d(k)\,\phi(k; \rho, \omega, \varphi)\right|^2$. Find the maximum of $\mathbf{\Gamma}(\rho, \omega, \varphi)$ and extract the parameters from $\Theta_{(\rho,\omega,\varphi)}$ as estimation of them, named $\hat{\rho}_d$, $\hat{\omega}_d$ and $\hat{\varphi}_d$. The maximum $\mathbf{\Gamma}\left(\hat{\rho}_d, \hat{\omega}_d, \hat{\varphi}_d\right)$ is treated as test statistic D for detection in the next step. It should be mentioned that top N maximum of $\mathbf{\Gamma}(\rho, \omega, \varphi)$ can be selected in order to obtain parameters of multiple targets simultaneously. Then N groups of estimation of parameters together with N numbers of test statistic will be used in sequence in the next step.

In the fourth step, compare the test statistic D with CFAR threshold obtained from the statistics of background energy

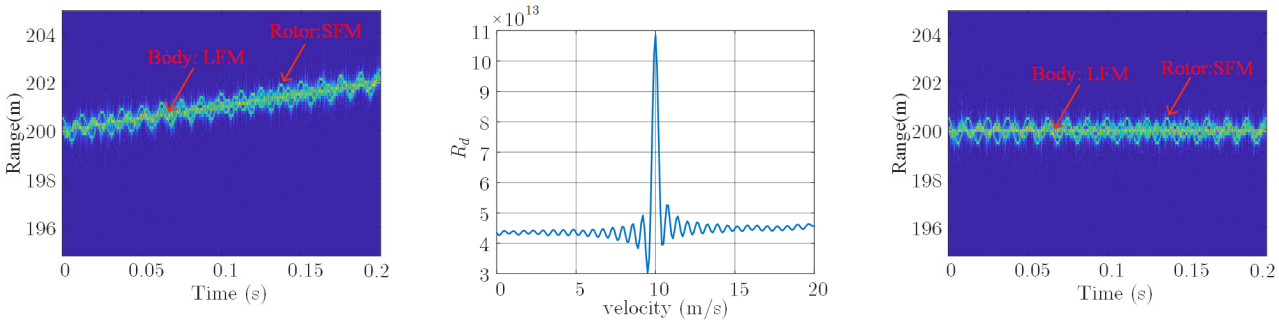

(a) (b) (c)

FIGURE 4. The result of the parametric space. (a) Range-time domain image of simulation target of four points (before translation compensation), (b) Relationship between accumulated energy R_d and test variable of translational velocity, (c) Range-time domain image of simulation target of four points (after translation compensation).

and make judgement. D being larger than the threshold means the existence of micro-motion target of rotor UAV, and less means non-existence. if the micro-motion target exists, calculate the rotor length $\hat{l}_d = \frac{\hat{\rho}_d \lambda}{4\pi}$ and rotation velocity $\hat{\omega}_d$ as micro-motion characteristics of rotor UAV for identification. Meanwhile, update the range of searching parameter space $\Theta_{(\rho,\omega,\varphi)}$ using $\hat{\rho}_d$, $\hat{\omega}_d$ and $\hat{\varphi}_d$ for the next iteration.

IV. EXPERIMENTS

A. SIMULATION

Suppose that the rotor UAV with four scattering points moves in the scene, the wavelength of radar signal is $\lambda = 0.0087m$, and the initial distance between target and radar is 200m. In order to access the parameters of rotor UAV commonly used on the market, the radius of rotation l, the rotational frequency ω_d and the initial rotation angle are shown in Table 1. The main body of UAV moves at the radial speed of $v_{d1} = 10m/s$. In addition, the simulation signal is added additive white Gaussian noise, which lead to an SNR $= 0dB$ echo data. The range-time domain image of the simulation echo signal after pulse compression is obtained and shown in Fig. 4. As can be seen in Fig. 4a, since UAV has the translational motion of the body and the rotation of the rotor at the same time, the echo is composed of two kinds of mixed signals, i.e. LFM component generated by translational motion and SFM component generated by micro motion. Meanwhile, the micro-Doppler amplitude of the four scattering points are magnified by a factor of $4\pi/\lambda$. Multiple micro-Doppler curves overlap each other in the cross-range unit, which brings difficulties to target feature extraction.

TABLE 1. Preset simulation parameters of four rotors.

Serial number	l_d (m)	$\frac{\omega_d}{2\pi}$ (r/s)	φ_d $(^\circ)$
1	0.1	100	0
2	0.2	95	30
3	0.3	90	60
4	0.5	80	90

Traditional parameter estimation method for a single component is no longer applicable. In this paper, the translational motion of the echo signal is needed to be compensated first. Based on the range dimension datashift method designed in section III-A, using (6)(7) to estimate the traditional velocity of rotor, we can obtain the relationship between accumulated energy R_d and test variable of translational velocity shown in Fig. 4b. That is, accumulated energy R_d reach the maximum when the test variable of translational velocity is $10m/s$ which turn out to be the translational velocity of the main body of rotor UAV. After compensating the translational motion of the echo, the range-time domain image of simulation target is shown in Fig. 4c.

Using the demodulator based on the maximum likelyhood criterion to find the maximum of test statistic D, the parameters of micro-Doppler model including micro-Doppler amplitude, angular frequency and initial phase are estimated, and the micro-motion targets are detected after CFAR detection. Searching matched micro-motion parameters in space $\Theta_{(\rho,\omega,\varphi)}$, we get four peaks of $\mathbf{\Gamma}(\rho,\omega,\varphi)$ shown in Fig. 5, and then the estimated result of micro-Doppler parameters of the four scattering point are shown in Table 2. The parameters of the four micro-Doppler components correspond to the four peak responses in the parameter space which can still obtain high precision of parameter estimation at low SNR.

TABLE 2. Result of parameter estimation of simulated four rotors.

Serial number	$\hat{l}_d$ (m)	$\frac{\hat{\omega}_d}{2\pi}$ (r/s)	$\hat{\varphi}_d$ $(^\circ)$
1	0.100	100.10	0.1
2	0.201	95.23	30.2
3	0.299	90.10	59.9
4	0.504	79.89	90.3

The effect of demodulator acted in the test statistic D can concentrate the energy of micro-Doppler components together into main component, which will increase the SNR of target with micro-Doppler characteristic for detection.

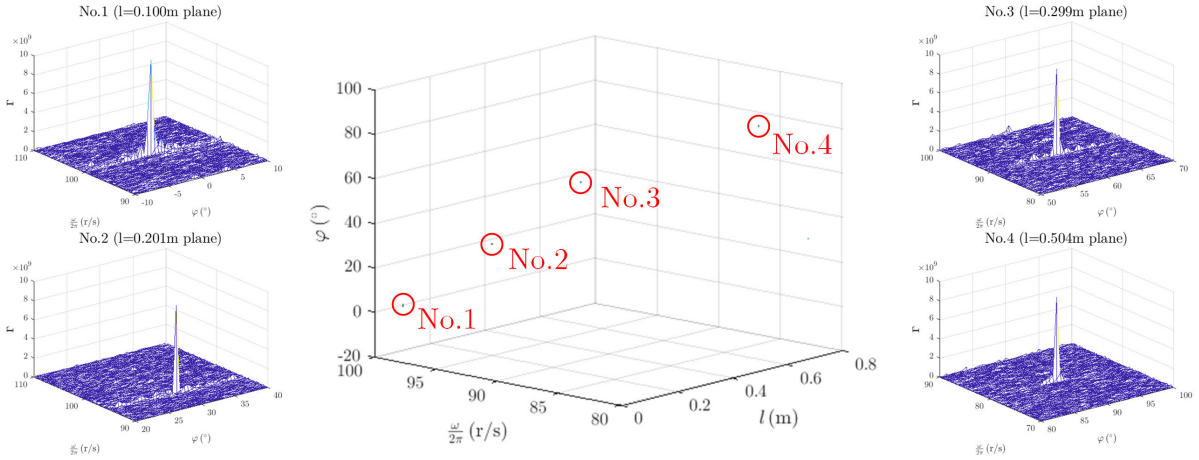

FIGURE 5. Results of four peaks of $\Gamma(\rho, \omega, \varphi)$ in space $\Theta_{(\rho,\omega,\varphi)}$.

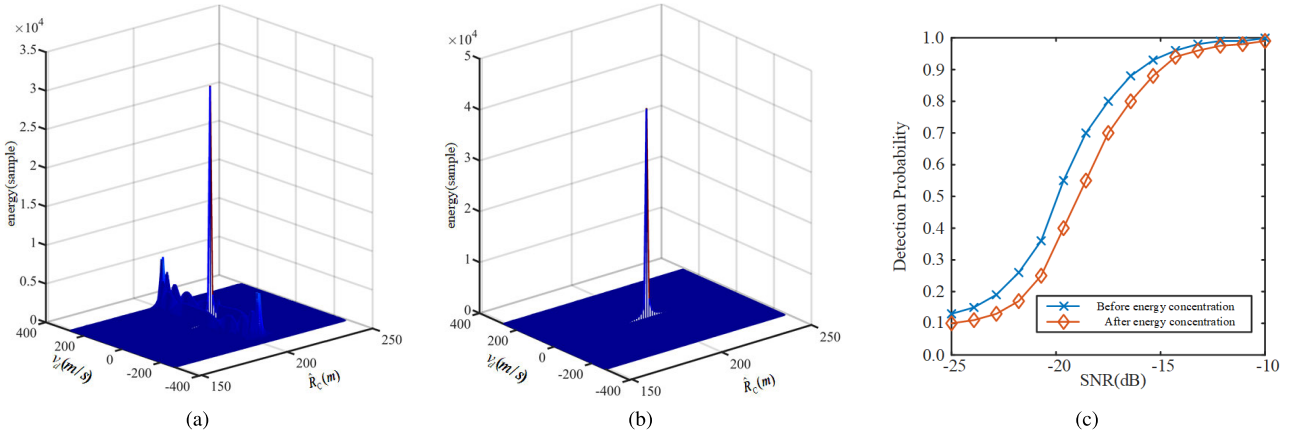

FIGURE 6. Comparison of results before and after energy concentration. (a) The result before energy concentration in range-Doppler(radial velocity) domain, (b) The result after energy concentration in range-Doppler(radial velocity) domain, (c) Comparison of detection probability of micro-motion target in different SNR circumstance before and after energy concentration.

Fig. 6 shows the comparison before and after energy concentration. The representation of energy concentration is shown in the range-Doppler(radial velocity) domain. In Fig. 6a, it is shown that the target can be concentrated in the same range gate, but the aggregation of the echo is not optimal due to the energy diffusion caused by micro-motion. In Fig. 6b, with the estimated result of micro-motion component of target, the energy can be concentrated in the same range gate and Doppler gate, and the energy concentration reach the highest level. from the processing simulation, the energy concentration of the target is increased about 1.3 times. Fig. 6c shows the comparison of the detection probability of micro-motion target in different SNR circumstance before and after energy concentration when fixing the false alarm probability with $P_{fa} = 10^{-6}$. It can be seen that when the echo of target obtained at SNR $= -15dB$, the detection probability with energy concentration is nearly 15% higher than that without energy concentration.

In order to compare the performance of different micro-motion target detection methods, we add Gaussian white noise with SNR from −40dB to 0dB to the radar echo of micro-motion target, and then 200 Monte Carlo experiments are carried out for each noise-added echo and each detection method. Here, we prefer HHT, FrFT, STFT-Hough and this-paper methods for comparison. The result of detection probability for each method is shown in Fig. 7. Because of the broadening effect caused by micro-motion, FrFT and other methods exhibit low precision in parameter search. Since the resolution of time and frequency cannot be obtained at the same time in STFT, the STFT-Hough estimation is not effective with limited computational cost. In this paper, the method of parameter estimation of micro-motion component based on maximum likelihood criterion demodulation operator has better anti-noise performance and estimation precision. In the low SNR circumstance, it can still achieve accurate target detection and parameter extraction performance.

B. REAL MEASURED DATA

In order to verify the effectiveness of this method in practical application, the experiment scenario is illustrated in Fig. 8.

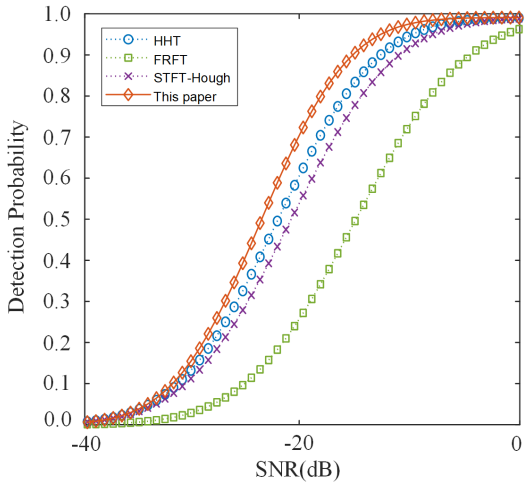

FIGURE 7. Detection performance of different methods with different SNR.

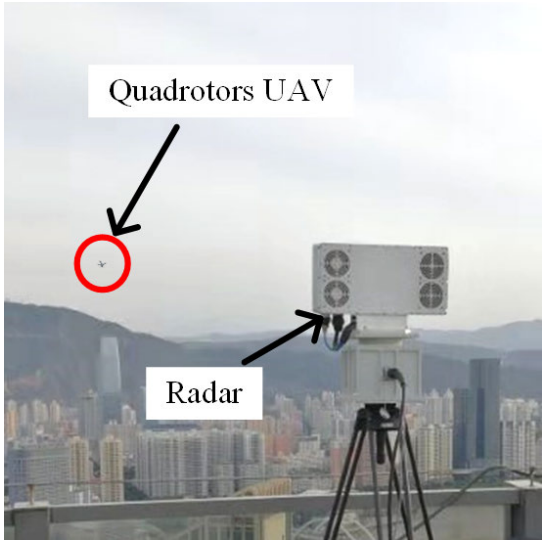

FIGURE 8. Experiment scenario.

TABLE 3. Parameters of radar system.

Parameter	Value
Central Frequency	34.6GHz
Bandwidth	1.2GHz
PRF	62.5kHz
Observation time	0.5s

In this image, a quad-rotor UAV (DJI-Spirit 3) is moving in the LOS direction of radar at the approximately speed of $15m/s$. Radar parameters are shown in Table 3.

In the experimental data, the stational clutter should be suppressed firstly because of the strong ground clutter such as trees in the field. In this paper, the method of pulse cancellation is used to suppress stational clutter. Then after pulse compression, the echo is shown in Fig. 9. As the effect of translational motion of the UAV body and micro-motion

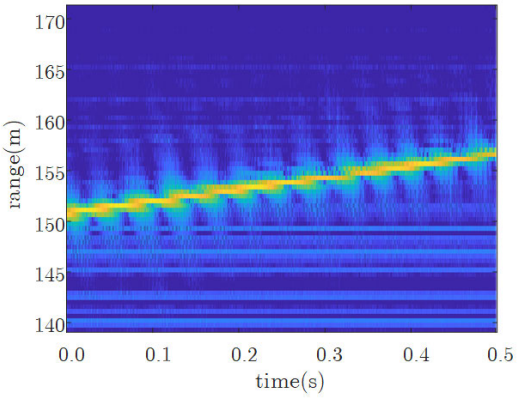

FIGURE 9. Range-slowtime domain image of measured echo signal after pulse compression.

of rotors, the target has a slant envelope shown as a range migration and periodic modulation shown as a periodic range extension.

Using range dimension datashift and demodulation processing in this paper to process the echo data, the parameters of main body and micro-motion of rotor UAV are estimated. Fig. 10a shows the results of target without micro-motion energy concentration in range-Doppler (radial velocity) domain after envelope compensation of translational component, which has strong anti-noise ability for translational energy extraction. It can be seen the concentrated translational component of UAV main body as the peak of the data, and its estimated translational velocity is shown as $\hat{v}_d = 12.74m/s$. Fig. 10b is a slice of Doppler domain corresponding to the position of target. It can be seen that there exists Doppler broadening because of the micro-Doppler components of each rotor which cause the micro-motion energy dispersion. After compensating the phase of translational component and demodulation of matched micro-motion parameters processing, two micro-motion components are estimated. Although there should be four rotors in the test UAV, two of them are blocked behind the radar line of sight without reflected echo. The other two are exposed to radar and their micro-motion parameters, namely the radius of rotation l and the rotational frequency ω, are expressed as $\hat{l}_{d1} = 0.130m$, $\hat{\omega}_{d1}/2\pi = 87.8r/s$ for the first rotor and $\hat{l}_{d2} = 0.128m$, $\hat{\omega}_{d2}/2\pi = 94.2r/s$ for the second one, which is basically in line with the actual situation of the test rotor UAV. It should be noted that the other micro-motion parameter namely initial rotation angle φ is stochastic and cannot be measured easily, so the estimation of this parameter cannot be compared to the real truth. Fig. 10c shows that by concentrating the micro-motion energy together onto the same position with main body in the Doppler domain, the SNR of target is increased. Fig. 10d is a slice of Doppler domain corresponding to the position of target. It shows the accumulation and enhancement result of target after energy concentration. The result shows that the

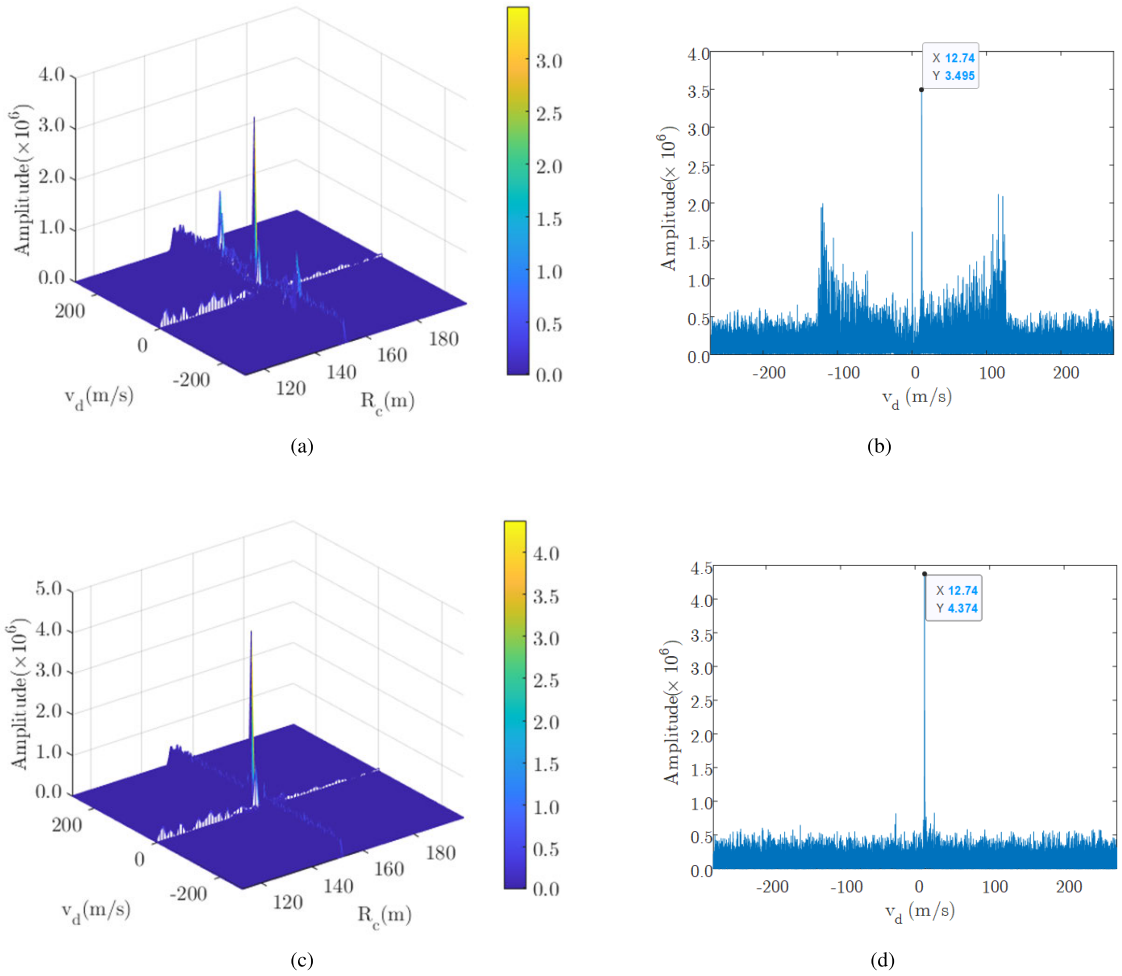

FIGURE 10. Comparison of results before and after energy concentration. (a) The result before energy concentration in range-Doppler(radial velocity) domain, (b) The slice of position of target range of (a) in Doppler(radial velocity) domain, (c) The result after energy concentration in range-Doppler(radial velocity) domain, (d) The slice of position of target range of (c) in Doppler(radial velocity) domain.

energy concentration of target is increased by 25.2%, which will improve the detect probability with constant false alarm rate. In conclusion, the experimental results show that this method has effective accuracy and feasibility for the detection of rotor UAV targets and estimation of micro-motion parameters.

V. CONCLUSION

Detection of rotor UAV with Low-slow-small feature is a significant problem for low-altitude air defense safety. Micro-Doppler is an important characteristic of rotor UAV. The precise estimation of Micro-Doppler parameters can be used to improve the performance of detection. In this paper, the micro-Doppler model of rotor UAV is established based on FMCW radar. Moreover, the phenomenon of broadening in the range direction caused by the micro motion of target is analyzed. Taking advantage of the characteristic differences of the signal components from the main body and the rotors in the echo, the LFM and SFM signals are processed by different methods. For the LFM signals modulated by the main body, a compensation method based on range dimension datashift is proposed. The motion parameters of the main body can be accurately estimated from the mixed signals, and the compensatory echo signal can create the condition for estimation of micro-motion parameters. For SFM signals modulated by rotors, a parameter estimation method for micro-Doppler signals based on the optimal estimation of demodulator is proposed by using the maximum likelihood method. the validity of the method and the detailed performance analysis are proved theoretically. Based on the optimal demodulator, the test statistics for micro-motion target detection is established, which obtain the highest level of discrimination between two hypotheses of existence and non-existence of micro-motion target. So the micro-motion target is detected with a high detection probability, and the micro-motion parameters are estimated accurately for the

identification. Finally, simulation and real measured data experiments indicate that the proposed method is effective in the detection of target with micro-Doppler information and the estimation of micro-motion parameters, and the characteristics formed by the micro-motion parameters could further be used for target classification and tracking.

In the follow-up research, we will study how to classify the suspicious and potentially dangerous targets from the information obtained, such as the structure of rotor, motion parameters, etc. Using these more refined features to identify the specific model of UAV, we can evaluate the level of its danger, so that we can formulate corresponding measures in advance to effectively avoid accidents. This work will have important significance for low altitude safety and protection.

APPENDIX A
DEDUCTION AND DEMONSTRATION OF EQUATION (24)

Let us derive the characteristics of D_1 in (23) and see it in (27), as shown at the bottom of the page.

According to Jacobi-Anger identity below:

$$\exp(jz\cos\theta) = \sum_{m=-\infty}^{+\infty} j^m J_m(z)\exp(jm\theta) = J_0(z) + 2\sum_{m=1}^{+\infty} j^m J_m(z)\exp(jm\theta), \quad (28)$$

we obtain the expression of D_1 in (29), as shown at the top of the next page, where ξ is the summation of product terms of Fourier expansions higher than first order acted as (30), as shown at the top of the next page. Equation (30) shows that ξ can be expressed as N point samplings on each product of high-order Fourier series term at intervals of Δt. Expanding the product of Fourier series term in ξ using product-to-sum identities of trigonometric function, we can get (31), as shown at the top of the next page. In (31), A is expressed as (32), as shown at the top of the next page. It can be seen from (31) that when N is large enough, the summation of each cosine term for k will form an accumulation when $\omega = \omega_d$ and

$$(m+n)\,\omega_d\,\Delta t = 2\pi q, \quad q \in \mathbb{Z}, \quad (33)$$

or

$$(m-n)\,\omega_d\,\Delta t = 2\pi q, \quad q \in \mathbb{Z}. \quad (34)$$

Otherwise, due to the positive and negative oscillation characteristics of the cosine function, the summation result approaches zero.

For (33) and (34), the conditions for forming the accumulation of cosine terms can be obtained as follows:

$$m + n = p\,\mathbf{lcm}\,(f_d, \mathrm{PRF})/f_d, \quad p \in \mathbb{N}^+, \quad (35)$$

or

$$m - n = p\,\mathbf{lcm}\,(f_d, \mathrm{PRF})/f_d, \quad p \in \mathbb{N}. \quad (36)$$

where, $f_d = \omega_d/2\pi$, $\mathrm{PRF} = 1/\Delta t$, $\mathbf{lcm}(\cdot)$ is the function of finding the least common multiple of two numbers. It is worth mentioning that if there are decimals in the two numbers of f_d and PRF on the right side of (35) and (36), the two numbers should be multiplied by the integer power of 10 at the same time, and the power level increase from 1 until the two numbers are both integers before the following proceeding.

According to the analysis above, when ξ is under the situation of $\omega = \omega_d$ and parameter m and n in each Fourier series term satisfying (35) or (36), there exists energy accumulation in ξ, which will cause interference and affect the estimation of micro-motion parameters.

The first term of D_1 in (29) takes the peak value when $\rho = \rho_d, \omega = \omega_d, \varphi = \varphi_d$, which is the correct estimation result of parameters. The interference term exists in ξ. From (35) and (36), combined with the properties of the first kind integer-order Bessel function, it can be seen that the position of interference in (ρ, ω, φ) space is a cluster of concentric circles on the plane $\omega = \omega_d$ with the center at point $(\rho_d, \omega_d, \varphi_d)$ and several series of rays on the plane $\omega = \omega_d$ passing through point $(\rho_d, \omega_d, \varphi_d)$ and some other points respectively. The interference energy on the rays decreases sharply as the distance from point $(\rho_d, \omega_d, \varphi_d)$ increases, which could be ignored for the reason of submerged under noise, so the main component of the interference is the cluster of concentric circles. The radius of each concentric circles is multiples of the circle with the smallest radius, and the length of the smallest radius is related to the PRF of the radar signal and the target parameter f_d which to be estimated. We use the interference energy on the circle with the smallest radius and the distance between it and point $(\rho_d, \omega_d, \varphi_d)$ (radius size) as an index to judge whether the interference affects the correct

$$\begin{aligned} D_1 &= \psi_d \sum_{k=0}^{N-1} \exp\left[j\rho_d \cos(\omega_d k\Delta t + \varphi_d)\right] \exp\left[-j\rho\cos(\omega k\Delta t + \varphi)\right] \\ &= \psi_d \sum_{k=0}^{N-1} \exp\left\{j\rho_d\left[\cos(\omega_d k\Delta t + \varphi_d) + \cos(\omega k\Delta t + \varphi - \pi)\right]\right\} \exp\left[j(\rho_d - \rho)\cos(\omega k\Delta t + \varphi)\right] \\ &= \psi_d \sum_{k=0}^{N-1} \exp\left[j2\rho_d \cos\left(\frac{\omega_d - \omega}{2}k\Delta t + \frac{\varphi_d - \varphi}{2} + \frac{\pi}{2}\right)\cos\left(\frac{\omega_d + \omega}{2}k\Delta t + \frac{\varphi_d + \varphi}{2} - \frac{\pi}{2}\right)\right] \\ &\quad \cdot \exp\left[j(\rho_d - \rho)\cos(\omega k\Delta t + \varphi)\right] \end{aligned} \quad (27)$$

$$D_1 = \psi_d \sum_{k=0}^{N-1} \left\{ \begin{array}{l} \left[\begin{array}{l} J_0\left(2\rho_d \cos\left(\frac{\omega_d-\omega}{2}k\Delta t + \frac{\varphi_d-\varphi}{2} + \frac{\pi}{2}\right)\right) \\ +2\sum_{m=1}^{+\infty} j^m J_m\left(2\rho_d \cos\left(\frac{\omega_d-\omega}{2}k\Delta t + \frac{\varphi_d-\varphi}{2} + \frac{\pi}{2}\right)\right)\cos\left(m\left(\frac{\omega_d+\omega}{2}k\Delta t + \frac{\varphi_d+\varphi}{2} - \frac{\pi}{2}\right)\right) \end{array} \right] \\ \cdot\left[J_0(\rho_d-\rho) + 2\sum_{n=1}^{+\infty} j^n J_n(\rho_d-\rho)\cos(n(\omega k\Delta t+\varphi))\right] \end{array} \right\}$$

$$= \psi_d \sum_{k=0}^{N-1} J_0\left(2\rho_d \cos\left(\frac{\omega_d-\omega}{2}k\Delta t + \frac{\varphi_d-\varphi}{2} + \frac{\pi}{2}\right)\right) J_0(\rho_d-\rho) + \xi \tag{29}$$

$$\xi = 4\psi_d \sum_{k=0}^{N-1} \left\{ \begin{array}{l} \sum_{m=1}^{+\infty} j^m J_m\left(2\rho_d \cos\left(\frac{\omega_d-\omega}{2}k\Delta t + \frac{\varphi_d-\varphi}{2} + \frac{\pi}{2}\right)\right)\cos\left[m\left(\frac{\omega_d+\omega}{2}k\Delta t + \frac{\varphi_d+\varphi}{2} - \frac{\pi}{2}\right)\right] \\ \cdot\sum_{n=1}^{+\infty} j^n J_n(\rho_d-\rho)\cos[n(\omega k\Delta t+\varphi)] \end{array} \right\}$$
$$+ 2\psi_d \sum_{k=0}^{N-1} \left\{ J_0\left(2\rho_d \cos\left(\frac{\omega_d-\omega}{2}k\Delta t + \frac{\varphi_d-\varphi}{2} + \frac{\pi}{2}\right)\right) \sum_{n=1}^{+\infty} j^n J_n(\rho_d-\rho)\cos[n(\omega k\Delta t+\varphi)] \right\}$$
$$+ 2\psi_d \sum_{k=0}^{N-1} \left\{ J_0(\rho_d-\rho) \sum_{m=1}^{+\infty} j^m J_m\left(2\rho_d \cos\left(\frac{\omega_d-\omega}{2}k\Delta t + \frac{\varphi_d-\varphi}{2} + \frac{\pi}{2}\right)\right)\cos\left[m\left(\frac{\omega_d+\omega}{2}k\Delta t + \frac{\varphi_d+\varphi}{2} - \frac{\pi}{2}\right)\right] \right\} \tag{30}$$

$$\sum_{k=0}^{N-1} \left\{ A\cos\left[m\left(\frac{\omega_d+\omega}{2}k\Delta t + \frac{\varphi_d+\varphi}{2} - \frac{\pi}{2}\right)\right]\cos[n(\omega k\Delta t+\varphi)] \right\}$$
$$= \sum_{k=0}^{N-1} \left\{ \begin{array}{l} \frac{A}{2}\cos\left[m\frac{\omega_d+\omega}{2}k\Delta t + n\omega k\Delta t + m\frac{\varphi_d+\varphi}{2} + n\varphi - m\frac{\pi}{2}\right] \\ +\frac{A}{2}\cos\left[m\frac{\omega_d+\omega}{2}k\Delta t - n\omega k\Delta t + m\frac{\varphi_d+\varphi}{2} - n\varphi - m\frac{\pi}{2}\right] \end{array} \right\} \tag{31}$$

$$A = \left\{ \begin{array}{ll} 2\psi_d j^{m+n} J_m\left(2\rho_d \cos\left(\frac{\omega_d-\omega}{2}k\Delta t + \frac{\varphi_d-\varphi}{2} + \frac{\pi}{2}\right)\right) J_n(\rho_d-\rho), & m=0 \textbf{ or } n=0 \\ 4\psi_d j^{m+n} J_m\left(2\rho_d \cos\left(\frac{\omega_d-\omega}{2}k\Delta t + \frac{\varphi_d-\varphi}{2} + \frac{\pi}{2}\right)\right) J_n(\rho_d-\rho), & \textbf{otherwise} \end{array} \right. \tag{32}$$

parameter estimation. Based on experience, the larger the least common multiple of f_d and PRF is, the larger the radius of the nearest circle to the point $(\rho_d, \omega_d, \varphi_d)$ in the concentric circle cluster is. Since the value of f_d cannot be predicted, we adopt the method of increasing PRF to enlarge the radius of the interference circles, thereby reducing the influence of interference on the correct parameter estimation. At this time, when (ρ, ω, φ) takes value near point (ρ, ω, φ), D_1 coule be expressed as

$$D_1 \doteq \psi_d \sum_{k=0}^{N-1} J_0\left(2\rho_d \cos\left(\frac{\omega_d-\omega}{2}k\Delta t + \frac{\varphi_d-\varphi}{2} + \frac{\pi}{2}\right)\right) J_0(\rho_d-\rho), \tag{37}$$

which is the same as (25).

REFERENCES

[1] Y. Zhao and Y. Su, "Sparse recovery on intrinsic mode functions for the micro-Doppler parameters estimation of small UAVs," *IEEE Trans. Geosci. Remote Sens.*, vol. 57, no. 9, pp. 7182–7193, Sep. 2019, doi: 10.1109/TGRS.2019.2912019.

[2] D. Hu, B. Qi, R. Du, H. Yang, J. Wang, and J. Zhuge, "An atmospheric vertical detection system using the multi-rotor UAV," in *Proc. Int. Conf. Meteorol. Observat. (ICMO)*, Chengdu, China, Dec. 2019, pp. 1–4, doi: 10.1109/ICMO49322.2019.9025899.

[3] W. C. Hsuan, L. S. Hao, and Y. C. Kuo, "Recognization of rice damage area on UAV ortho-images," in *Proc. IEEE Int. Conf. Appl. Syst. Invention (ICASI)*, Chiba, Japan, Apr. 2018, pp. 1092–1094, doi: 10.1109/ICASI.2018.8394470.

[4] Q. Sun, H. Li, Y. Zhang, Y. Xie, and C. Liu, "A baseline assessment method of UAV swarm resilience based on complex networks," in *Proc. IEEE 19th World Symp. Appl. Mach. Intell. Informat. (SAMI)*, Herl'any Slovakia, Jan. 2021, pp. 83–86, doi: 10.1109/SAMI50585.2021.9378640.

[5] J. P. Yaacoub, H. Noura, O. Salman, and A. Chehab, "Security analysis of drones systems: Attacks, limitations, and recommendations," *Internet Things*, vol. 11, Sep. 2020, Art. no. 100218, doi: 10.1016/j.iot.2020.100218.

[6] S. A. Musa, R. S. A. R. Abdullah, A. Sali, A. Ismail, and N. E. A. Rashid, "Low-slow-small (LSS) target detection based on micro Doppler analysis in forward scattering radar geometry," *Sensors*, vol. 19, no. 15, pp. 3332-1–3332-20, Jul. 2019, doi: 10.3390/s19153332.
[7] F. Fioranelli, M. Ritchie, H. Griffiths, and H. Borrion, "Classification of loaded/unloaded micro-drones using multistatic radar," *Electron. Lett.*, vol. 51, no. 22, pp. 1813–1815, Oct. 2015, doi: 10.1049/el.2015.3038.
[8] D. Tahmoush, "Review of micro-Doppler signatures," *IET Radar, Sonar Navigat.*, vol. 9, no. 9, pp. 1140–1146, Dec. 2015, doi: 10.1049/iet-rsn.2015.0118.
[9] Y. Wang, C. Feng, Y. Zhang, and S. He, "Translational motion compensation of space micromotion targets using regression network," *IEEE Access*, vol. 7, pp. 155038–155047, 2019, doi: 10.1109/ACCESS.2019.2947277.
[10] S. Rahman and D. A. Robertson, "Radar micro-Doppler signatures of drones and birds at K-band and W-band," *Sci. Rep.*, vol. 8, no. 1, p. 17396, Nov. 2018, doi: 10.1038/s41598-018-35880-9.
[11] L. Hong, X. Wang, and S. Liu, "Micro-Doppler curves extraction based on high-order particle filter track-before detect," *IEEE Geosci. Remote Sens. Lett.*, vol. 16, no. 10, pp. 1550–1554, Oct. 2019, doi: 10.1109/LGRS.2019.2904581.
[12] F.-F. Gu, M.-H. Fu, B.-S. Liang, K.-M. Li, and Q. Zhang, "Translational motion compensation and micro-Doppler feature extraction of space spinning targets," *IEEE Geosci. Remote Sens. Lett.*, vol. 15, no. 10, pp. 1550–1554, Oct. 2018, doi: 10.1109/LGRS.2018.2849869.
[13] Y. Xing, P. You, H. Wang, S. Yong, and D. Guan, "Adaptive translational motion compensation method for rotational parameter estimation under low SNR based on HRRP," *IEEE Sensors J.*, vol. 19, no. 7, pp. 2553–2561, Apr. 2019, doi: 10.1109/JSEN.2018.2889752.
[14] L. Ren, N. Tran, F. Foroughian, K. Naishadham, J. E. Piou, O. Kilic, and A. E. Fathy, "Short-time state-space method for micro-Doppler identification of walking subject using UWB impulse Doppler radar," *IEEE Trans. Microw. Theory Techn.*, vol. 66, no. 7, pp. 3521–3534, Jul. 2018, doi: 10.1109/TMTT.2018.2829523.
[15] B. O. Bozdag and I. Erer, "A comparative study on micro-Doppler signature generation methods for UAVs using rotor blade model," in *Proc. 6th Int. Conf. Electr. Electron. Eng. (ICEEE)*, Istanbul, Turkey, Apr. 2019, pp. 298–301, doi: 10.1109/ICEEE2019.2019.00064.
[16] S. Huixia and S. Shidong, "Micro-Doppler frequency estimation based on Radon-Wigner transform," *Defence Sci. J.*, vol. 64, no. 1, pp. 85–87, Jan. 2014, doi: 10.14429/dsj.64.2980.
[17] P. Li, D.-C. Wang, and J.-L. Chen, "Parameter estimation for micro-Doppler signals based on cubic phase function," *Signal, Image Video Process.*, vol. 7, no. 6, pp. 1239–1249, Nov. 2013, doi: 10.1007/s11760-012-0395-0.
[18] X. Chen, J. Guan, Z. Bao, and Y. He, "Detection and extraction of target with micromotion in spiky sea clutter via short-time fractional Fourier transform," *IEEE Trans. Geosci. Remote Sens.*, vol. 52, no. 2, pp. 1002–1018, Feb. 2014, doi: 10.1109/TGRS.2013.2246574.
[19] P. Suresh, T. Thayaparan, T. Obulesu, and K. Venkataramaniah, "Extracting micro-Doppler radar signatures from rotating targets using Fourier-Bessel transform and time–frequency analysis," *IEEE Trans. Geosci. Remote Sens.*, vol. 52, no. 6, pp. 3204–3210, Jun. 2014, doi: 10.1109/TGRS.2013.2271706.
[20] C. Pang, Y. Han, H. Hou, S. Liu, and N. Zhang, "Micro-Doppler signal time-frequency algorithm based on STFRFT," *Sensors*, vol. 16, no. 10, pp. 1559-1–1559-17, Oct. 2016, doi: 10.3390/s16101559.
[21] C. Cai, W. Liu, J. S. Fu, and Y. Lu, "Radar micro-Doppler signature analysis with HHT," *IEEE Trans. Aerosp. Electron. Syst.*, vol. 46, no. 2, pp. 929–938, Apr. 2010, doi: 10.1109/TAES.2010.5461668.
[22] Q. Changwen, W. Ying, C. Botao, and S. Feng, "Using a FMCW SAR to image the corner-reflector," in *Proc. 9th Int. Conf. Signal Process.*, Beijing, China, Oct. 2008, pp. 2267–2270, doi: 10.1109/ICOSP.2008.4697601.
[23] Y. Hu, Y. Zhang, J. Sun, and P. Lei, "Focusing vibrating targets in frequency-modulation continuous-wave-synthetic aperture radar with Doppler keystone transform," *J. Appl. Remote Sens.*, vol. 10, no. 2, Jun. 2016, Art. no. 025019, doi: 10.1117/1.JRS.10.025019.
[24] J. Xu, J. Yu, Y.-N. Peng, and X.-G. Xia, "Radon-Fourier transform for radar target detection, I: Generalized Doppler filter bank," *IEEE Trans. Aerosp. Electron. Syst.*, vol. 47, no. 2, pp. 1186–1202, Apr. 2011, doi: 10.1109/TAES.2011.5751251.
[25] X. Rao, H. H. Tao, J. Su, X. L. Guo, and J. Z. Zhang, "Axis rotation MTD algorithm for weak target detection," *Digit. Signal Process.*, vol. 26, pp. 81–86, Mar. 2014, doi: 10.1016/j.dsp.2013.12.003.
[26] Y. He, J. Guan and X. Meng, *Radar Target Detection and CFAR Processing*, 2nd ed. Beijing, China: Tsinghua Univ. Press, 2011, pp. 36–68.

GUANGYU JI was born in Shenyang, Liaoning, China, in 1988. He received the B.S. degree in electronic information engineering from the University of Science and Technology of China, Hefei, China, in 2011, and the Ph.D. degree in signal and information processing from the University of Chinese Academy of Sciences, Beijing, China, in 2018.

He is currently a Postdoctor with the People's Public Security University of China, Beijing. His research interests include radar system design, radar target detection algorithm design, and radar signal processing.

CHEN SONG was born in Jinzhong, Shanxi, China, in 1992. He received the B.S. degree in electronic information engineering from Harbin Engineering University, Harbin, China, in 2015, and the Ph.D. degree in signal and information processing from the University of Chinese Academy of Sciences, Beijing, China, in 2020.

He is currently an Assistant Researcher with the Aerospace Information Research Institute, Chinese Academy of Sciences, Beijing. His research interests include radar system design, radar image processing, radar micro-Doppler, and digital signal processing.

HONGTAO HUO (Member, IEEE) received the M.S. and Ph.D. degrees in computer science and technology from Beijing Forestry University, Beijing, China, in 1998 and 2001, respectively.

He is currently a Professor with the Department of Information Technology and Cyber Security, People's Public Security University of China, Beijing. His research has been supported by the National Key Research and Development Program of China and the Ministry of Public Security Technology Research Program. He has published several articles in various refereed journals. His research interests include image processing and pattern recognition, remote sensing application technology, and image forensics.